Journal Pre-proof

Development of Sandwich Chemiluminescent Immunoassay based on an Anti-Staphylococcal enterotoxin B Nanobody–Alkaline Phosphatase Fusion Protein for Detection of Staphylococcal Enterotoxin B

Tieqiang Sun, Zunquan Zhao, Wentao Liu, Zehua Xu, Hongwei He, Baoan Ning, Yongqiang Jiang, Zhixian Gao

PII: S0003-2670(20)30068-4

DOI: https://doi.org/10.1016/j.aca.2020.01.032

Reference: ACA 237392

To appear in: *Analytica Chimica Acta*

Received Date: 17 September 2019

Revised Date: 18 December 2019

Accepted Date: 15 January 2020

Please cite this article as: T. Sun, Z. Zhao, W. Liu, Z. Xu, H. He, B. Ning, Y. Jiang, Z. Gao, Development of Sandwich Chemiluminescent Immunoassay based on an Anti-Staphylococcal enterotoxin B Nanobody–Alkaline Phosphatase Fusion Protein for Detection of Staphylococcal Enterotoxin B, *Analytica Chimica Acta*, https://doi.org/10.1016/j.aca.2020.01.032.

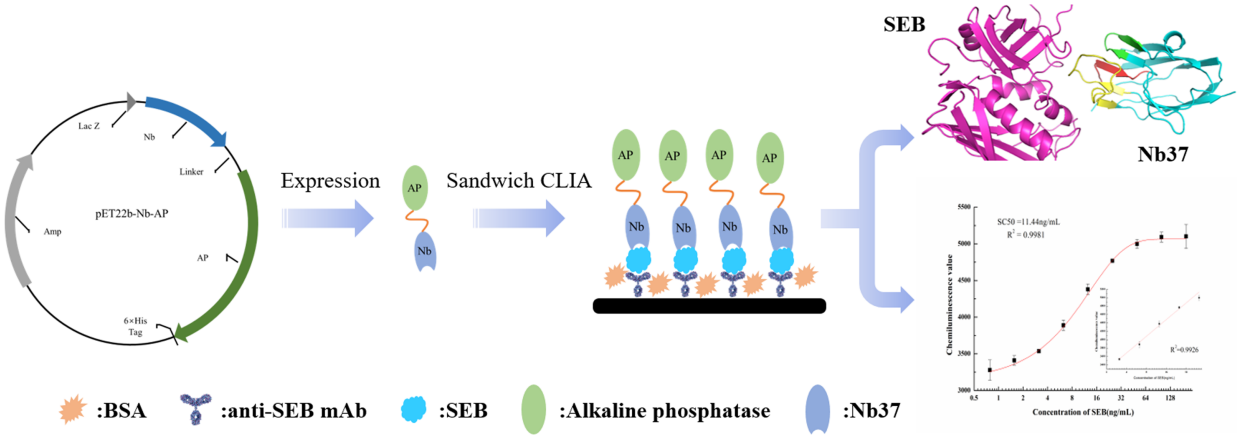

Development of Sandwich Chemiluminescent Immunoassay based on an Anti-Staphylococcal enterotoxin B Nanobody–Alkaline Phosphatase Fusion Protein for Detection of Staphylococcal Enterotoxin B[1]

Tieqiang Sun[1], Zunquan Zhao[2], Wentao Liu[3], Zehua Xu[1], Hongwei He[1], Baoan Ning[1*], Yongqiang Jiang[2]*, Zhixian Gao[1]*

[1]Tianjin Key Laboratory of Risk Assessment and Control Technology for Environment & Food Safety, Tianjin Institute of Environmental and Operational Medicine, Tianjin, 300050, China

[2]State Key Laboratory of Pathogens and Biosecurity, Institute of Microbiology and Epidemiology, Beijing 100071, China

[3] College of public health, Inner Mongolia Medical University, Hohhot, 010059, China

[*]**Joint correspondence to:**

Zhixian Gao

Tianjin Key Laboratory of Risk Assessment and Control Technology for Environment & Food Safety, Tianjin Institute of Environmental and Operational Medicine, No. 1 Dali Road, Tianjin 300050, China;
E-mail: gaozhx@163.com; Telephone and fax numbers: +86-022-84655192;

Yongqiang Jiang

State Key Laboratory of Pathogens and Biosecurity, Institute of Microbiology and Epidemiology, Beijing 100071, China
E-mail: jiangyq@nic.bmi.ac.cn;

Baoan Ning

Tianjin Key Laboratory of Risk Assessment and Control Technology for Environment & Food Safety, Tianjin Institute of Environmental and Operational Medicine, No. 1 Dali Road, Tianjin 300050, China;

E-mail: ningba@163.com; Telephone and fax numbers: +86-022-84655192.

[1] Table of abbreviation

BSA Bovine serum albumin

ELISA Enzyme-labeling for second antibodies and to reduce the procedure time of enzyme-linked immunosorbent assay

LB Lysogeny broth

LOD Limit of detection

MHC Major histocompatibility complex

OD Optical density

PBS Phosphate-buffered saline

PDB Protein Data Bank

TcR T-cell receptor-

Highlights:

Nanobodies that bind to SEB were isolated from a naïve library,

The molecular mechanism of nanobodies interacting with SEB was described,

Nb37–ALP has the potential to replace chemically-coupled detection antibodies,

Nb37–ALP was shown to be thermally stable and be able to be produced in large scale,

A quick and sensitive sandwich CLIA method for the detection of SEB was developed.

Abstract

In this study, sandwich chemiluminescent immunoassay (CLIA) for the detection of Staphylococcal enterotoxin B (SEB) was developed using nanobody–alkaline phosphatase (Nb–ALP) fusion protein. The SEB-binding nanobodies were obtained from a naïve phage-display library and the Nb–ALP fusion protein was constructed and obtained as a thermally stable and potentially effective substance for detecting antibodies in CLIA. The working range of the sandwich CLIA based on anti-SEB monoclonal antibodies (mAbs) and our fusion protein, Nb37–ALP, was 3.12–50.0 ng mL^{-1} with SC50 = 8.59 ± 0.37 ng mL^{-1}. The limit of detection was 1.44 ng mL^{-1} according to the blank value plus 3 standard deviations. In order to understand the interaction of SEB and Nb37 in depth, the 3D structure of the SEB–Nb37 complex was constructed and verified by molecular modeling and the docking method. The results showed that the complementary-determining region 3 (CDR3) of Nb37 embedded itself in the opening generated by the major histocompatibility complex (MHC) and T-cell receptor- (TcR) binding sites of SEB, indicating that Nb37 may affect the recognition of SEB by MHC class □ molecules and the TcR. The arginine residue (Arg) 101, Arg102 and phenylalanine residue (Phe)103 of CDR3 in Nb37 may have contributed to specific binding to form six salt-bridges between these and SEB. In conclusion, in terms of their specificity and sensitivity, the obtained anti-SEB Nb–ALP appears to have the potential to replace chemically labeled probes for the detection of SEB.

Keywords: Nanobody; Staphylococcal Enterotoxin B; Alkaline Phosphatase; Immunoassay.

1 Introduction

Recently, harmful bacteria have been the most common cause of foodborne disease, which has been one of the biggest issues affecting human health and food safety [1]. Among these illnesses, Staphylococcal food poisoning is the second most frequently reported [2]. Staphylococcal enterotoxin B (SEB), which causes burn sepsis and staphylococcal toxic shock syndrome, is considered to be one of the most important virulence factors of the disease [3]. The half lethal dose (LD50) of SEB is around 20 ng/kg, but the enterotoxin leads to poisoning even when taken at 0.4 ng/kg [4]. As SEB represents a huge threat to human health and food safety, the development of a simple, sensitive, and quantitative method for the detection of SEB is desirable.

Immunoassay based on antibody-antigen recognition is the method most often used for the detection of SEB [5-7]. Immunoassay is simple, sensitive and economic, and is currently the most important tool for the detection of SEB. The most common reported immunoassay method used for SEB is sandwich immunoassay, which requires the capture and detection of antibodies. To avoid the use of enzyme-labeling for second antibodies and to reduce the procedure time of enzyme-linked immunosorbent assay (ELISA), the detected antibodies are usually chemically labeled with enzymes [8-10] or nanoparticles [6, 11-13]. However, the chemical combination of nanoparticles or reporter antibodies may result in a loss of antibody activity and instability from batch to batch [14, 15].

Nanobodies derived from camel heavy-chain antibodies are the smallest recombinant antibodies (approximately 15 kDa). Due to their long and protruding complementary-determining region 3 CDR3 loop, they can reach hidden (cryptic) and concave epitopes [16]. Further, nanobodies are endowed with unique physical and chemical advantages over conventional antibodies, such as high tolerance to temperatures, proteases, solvents and pH [17-19]. At the same time, nanobodies have a similar performance to conventional antibodies when binding to their cognate antigen [20]. Nanobodies also have a higher solubility and higher expression in microbial systems compared with conventional antibodies [21]. Because of their high affinity and low molecular weight, nanobodies are also easy to clone and derivatize by coupling to reporter protein [22]. These recombinant fusion proteins can be developed into one-step immunoassay methods that avoid the incubation time of secondary antibodies. Many one-step immunoassay methods have been constructed using the fusion of alkaline phosphatase (ALP) to nanobodies, such as fumonisin B1 [23], porcine circovirus type 2 [24] and ochratoxin A [25].

In this study, we isolated a SEB nanobody from a naïve nanobody phage-display library, constructed Nb–ALP fusion protein, and expressed it in *Escherichia coli* Origami B(DE3) cells. Then, a chemiluminescent immunoassay (CLIA) method using Nb–ALP was developed for quick and sensitive detection of SEB.

2 Materials and Methods

2.1 Materials and Reagents

The Staphylococcal enterotoxins SEA and SEB were purchased from Hongxin Co., Ltd (Hangzhou, China). Peroxidase-labeled anti-M13 phage antibody was obtained from GE Healthcare (Piscataway, USA). Anti-6×His antibody coupled to peroxidase and a nickel- (Ni) affinity chromatography column were purchased from Sangon Biotech (Shanghai, China). Isopropyl-β-D-thiogalactoside (IPTG), ovalbumin (OVA) and bovine serum albumin (BSA) were obtained from Sigma Aldrich (St. Louis, USA). A GenBuilder DNA Assembly Kit was purchased from GenScript (Nanjing, China). Alkaline phosphatase substrate (AMPPD) was purchased from Maxchemtech (Shenzhen, China). Restriction

enzymes EcoR I, Hind III, T4 DNA ligase and Q5 High-Fidelity DNA Polymerase were purchased from New England Biolabs Ltd. (Beijing, China). The pET-22b vector, *E coli* Origami B(DE3), was purchased from Novagen (Darmstadt, Germany). The chemiluminescence immunoanalyzer was procured from Tigun Inc. (Beijing, China). Transparent microplates were purchased from Jet Bio-Filtration Co., Ltd. (Guangzhou, China), and the white microplates for luminescence assays were purchased from Thermo Fisher Scientific Inc. (Shanghai, China). All chemicals were of the analytical grade.

2.2 Selection of Phage-Display Nanobodies for SEB

A naïve phage-display nanobody library was constructed according to the phage-display technology manuals [26] for the selection of SEB-binding nanobodies. A biopanning procedure was carried out that included five rounds of panning in immune tubes. Antigen SEB was coated at 10, 5, 2.5 , 1, and 0.5 μg in 1 ml phosphate-buffered saline (PBS) and incubated at 4 ℃ for 12 h. 2 ml 3% BSA and 2 ml 3% OVA in PBS were alternately used to block the immune tube for 1 h at 37 ℃. 10 washings were carried out with 0.05% PBST (Tween-20, v/v%). Then, 500 μL of naïve phage-display nanobody library was preincubated with 500 μL 3% BSA and 500 μL 3% OVA in PBS for 30 min at 37 ℃ to discard nonspecific phages. Then, the library was added into the tube for 1 h at 37 ℃. Nonbinding phages were discarded using 10 washing cycles with 0.1% PBST (Tween-20, v/v%). Then, 1 ml 0.1 M hydrochloric acid (HCl; pH 2.0) was added into the tube and incubated for 8 min at 37 ℃ to elute binding phages, and 0.5 ml 1 M Tris-HCl (pH 9.0) was added to neutralize the elution buffer immediately. 10 μL of the elution solution from each round was used to test the phage titer and the remainder was amplified for the following biopanning. After the five-round biopanning, phage-ELISA was performed to select SEB-binding phages and the genes of positive clones were sequenced for further characterization.

2.3 Expression and Purification of Soluble Anti-SEB Nanobodies

The genes of positive nanobodies were subcloned into expression vector pET-22b(+) using the DNA assembly kit according to the manual. The recombinant plasmids were then transformed into *E.coli Origami* B(DE3)-competent cells, and a single colony was picked and cultured in a lysogeny broth (LB) medium, containing 100 μg ml^{-1} each of ampicillin, kanamycin, and tetracycline.

Expression of soluble nanobodies was carried out by adding 0.4 mM IPTG into the LB medium at OD600 = 0.6 and incubating this for another 12 h at 18 ℃. The medium was then centrifuged for 20 min at 3500 *g* at 4 ℃. To obtain crude extract, the lysates which were lysed by ultrasonic cell disruption were centrifugated at 8000 g for 20 min. The supernatant was then purified using Ni-affinity columns, and the target proteins were analyzed by SDS-PAGE.

2.4 Characterization of Nanobody Binding

Direct ELISA was used to evaluate the character of purified nanobodies. Briefly, 100 μL of serially diluted SEB was added to microwells and incubated at 4 ℃ overnight. Then, 120 μL 1% BSA in PBS was added into the plate and incubated for 1 h at 37 ℃. Purified nanobodies in PBST were next added and incubated for 1 h at 37 ℃. A washing step was carried out three times using PBST, and 100 μL anti-His immunoglobin G-horseradish peroxidase (IgG-HRP) was added and incubated at 37 ℃ for another 1 h. After this step, 100 μL TMB solution was added and the plate was incubated for 15 min at 37 ℃. The reaction was finally stopped by the addition of 50 μL 2 M sulfuric acid (H_2SO_4), and the optical density (OD) of the solution was measured at 450 nm by a microplate reader (Molecular Devices).

To understand the interaction between SEB and the best SEB-binding nanobody, Nb37, the three-dimensional structures of Nb37 was modeled using MODELLER [27, 28]. The three-dimensional structure of SEB was downloaded from the Protein Data Bank (PDB) [29]. After the potential energies of the modeled structure had been separately minimized, the interaction between SEB and Nb was predicted by RosettaDock [30]. A visualization of the interaction between SEB and Nb37 was created using PyMOL [31, 32].

2.5 Construction and Expression of Soluble Nb37–ALP

Nb37–ALP fusion protein was constructed by fusing Nb37, (G4S)3 linker and ALP (derived from *E. coli*) by SOC-PCR[33, 34]. A substitution serine for Asp101 in the gene of ALP was introduced and led to a 35-fold increase of specific activity [35]. The gene of the fusion protein was then cloned into pET-22b as described above. The pET-22b–Nb–ALP plasmid was used in *E.coli* Origami B(DE3). The expression and purity of Nb37–ALP were determined as described above.

2.6 Sandwich CLIA for SEB based on Nb37–ALP

1 μg ml^{-1} anti-SEB mAb was incubated at 4 □ overnight. The coated plates were blocked as described above, and after washing, 100 μL of SEB standard in PBS was added and incubated for 1 h at 37 □. The plate was then incubated again with 100 μL Nb–ALP in PBST. Next, the AP enzyme activity was revealed by the addition of 100 μL AMPPD substrate. Light emission was then measured using a chemiluminescence immunoanalyzer (Tigun, Beijing China).

2.7 Cross-reactivity and Thermostability

To determine the selectivity of the Nb37–ALP fusion protein, sandwich CLIA was carried out using SEB-similar protein. SEA, SEB, BSA, OVA and mouse IgG at 50 ng mL^{-1} in PBS were used to measure the specificity of the sandwich CLIA.

The Nb37–ALP in PBS was incubated separately at 37 □, 60 □ and 80 □ for 90 min, and the activity of the Nb37–ALP was tested at 0, 30, 60, and 90 min using sandwich CLIA. Briefly, 1 μg mL^{-1} anti-SEB mAb was incubated at 4 □ overnight. The next day, washing and blocking steps were carried out as described above. 100 μL 50 ng mL^{-1} SEB in PBS was added after the washing step and incubation was carried out, also as described above. Then, the SEB–Nb37–ALP was added and incubated for 1 h at 37 □. Next, 100 μL AMPPD substrate was added and the signal was recorded using a chemiluminescence immunoanalyzer (Tigun, Beijing China).

2.8 Recovery Analysis of Spiked Samples

To evaluate the reliability of this method in a real sample, whole milk, drinking water (bought from a local market) and fresh human serum (collected from a healthy volunteer) were selected as spiked samples. First, the original concentration of SEB was detected using a commercial ELISA kit (Jianglai Biological, China). Then, different amounts SEB was added to these samples to final concentrations of 5, 10, 20 and 40 ng mL^{-1}. Before testing, the spiked samples were centrifuged at 8000 *g* for 20 min to remove fat. Then, 100 μL supernatant of the samples were analyzed using both CLIA and a commercial ELISA kit. The measurement of each sample was performed in duplicate three times.

3 Results and Discussion

3.1 Selection of Phage-Display Nanobody against SEB

A naïve phage-display nanobody library was used to select SEB-binding nanobodies. To obtain SEB-binding nanobodies, we utilized the biopanning strategy, decreasing the concentration of immobile SEB and increasing selection pressure. Five cycles of panning were carried out according to the

enrichment of specific phage nanobodies. For each cycle, the recovery rate was calculated by comparing the output titer to the input titer of phage nanobodies, while the enrichment was calculated by comparing the recovery rates of each round to the one preceding it. After biopanning, the enrichment of SEB-binding nanobodies had increased, remarkably, to 4.11 (Figure 1). Forty-eight clones were then randomly selected from the fifth round of panning and subjected to monoclonal phage ELISA to identify SEB-binding clones. Among them, 13 positive clones that showed specific binding to SEB, but not to BSA, were identified (Figure 2). Sequence alignment results revealed that the 13 clones had four nanobody sequences, collectively (Figure 3). The framework regions of the four clones demonstrated high conservation with one another. Characteristic substitutions (F48, E55, R56, and F/G58) of the nanobodies in FR2 were observed in the four clones, which indicates that all of these nanobodies were derived from heavy-chain camelid antibodies [21, 36].

3.2 Expression and Purification of Soluble Anti-SEB Nanobodies

For expression of nanobodies, the genes of four unique nanobodies were subcloned into pET-22b and the recombinant plasmids were transformed into *E. coli* Origami B(DE3). Nanobodies were obtained using Ni-affinity chromatography columns from the supernatant of lysed cells. To characterize the purity of nanobodies, SDS-PAGE electrophoresis was carried out. Figure 4 shows the theoretical size of nanobodies calculated by BioEdit and the four nanobodies of about 17 kDa that were detected.

3.3 Characterization of Nanobody **Binding**

Direct ELISA was used to estimate the sensitivity of the nanobodies. As shown in Figure 5, 50% of maximal signals (SC_{50}) for Nb13, Nb16, Nb23, and Nb37 were 22.7 ng mL^{-1}, 83.3 ng mL^{-1}, 28.7ng mL^{-1} and 19.3ng mL^{-1}, respectively. Among them, Nb37 showed better binding activity than other nanobodies with smaller SC50. Thus, Nb37 was selected to dock with SEB in silico and create the Nb–ALP fusion protein.

To understand the interaction between SEB and Nb37, a 3D model of Nb37 was generated using MODELLER and the 3D structure of SEB was downloaded from the PDB. The SEB–NB37 structure (Figure 6a, 6b) was predicted using RosettaDock. According to the docking prediction, the CDR3 of Nb37 embedded itself in the opening generated by the MHC- and TcR-binding sites of SEB, indicating that Nb37 has the ability affect the recognizability of SEB to the MHC class □ and TcR receptors. The interaction analysis (Figure 6c) revealed that hydrophobic and electrostatic interactions present at the binding interface determined the high specificity and high affinity. The Arg101, Arg102, and Phe103 of Nb37 formed six salt-bridges with the Val152, Asn157, and Asn186 of SEB, which were pivotal for the specificity of complex formation.

3.4 Construction and Expression of Nb37–ALP

The construction of pET-22b–Nb–ALP is shown in Figure 7. The positive recombinant plasmid was confirmed by Sanger sequencing, and the correct plasmid was transformed into *E.coli* Origami B(DE3). A single colony was the selected from the LB agar plate and cultured at 37 □ and at 200 rpm in a shaking incubator. When the OD600 value of the culture reached between 0.4 and 0.6, IPTG (0.4 mM) was added to induce the expression of the Nb–ALP fusion protein. After purification by Ni-affinity chromatography column, the Nb–ALP fusion was analyzed using SDS-PAGE (Figure 8). The SDS-PAGE analysis showed that the fusion protein was soluble and had a band of approximately 70 kDa, as expected.

3.5 Sandwich CLIA for SEB based on Nb37–ALP

Using anti-SEB mAb as a capture antibody and Nb37–ALP as a detector antibody, sandwich CLIA was developed for SEB detection. After optimization, the optimal concentrations of the capture antibody and detection antibody were determined using the checkboard method. Figure 9 shows the sandwich CLIA developed with the optimal concentrations of anti-SEB mAb and Nb37–ALP. The working range of the assay was defined as the part of the curve with a linear coefficient of $R^2 > 0.99$. The linear range was from 3.12–50.00 ng mL^{-1} with SC_{50} = 8.59 ± 0.37 ng mL^{-1}. The limit of detection, defined as the blank value plus 3 standard deviations, was 1.44 ng mL^{-1}. Table 1 shows a brief overview of the immunoassay for SEB detection. To enhance their sensitivity, these methods would all require complex chemical modification that would lead a difference between batches as well as higher costs. With regard to the criterion for the pathogeny of food poisoning, the U.S. Food and Drug Administration defines as 1 mg SEs intake equal to take 100 ng mL^{-1} SEs in 10 mL of contaminated milk. And the LOD determined by the ELISA is 1.25 ng mL^{-1}, as published by General Administration of Quality Supervision, Inspection and Quarantine of the People's Republic of China. These indicate that our method would meet the testing requirements established by both of these standards.

Table 1 Immunoassays reported in the literature for the detection of SEB

No	Mechanism	Detection Limit (ng mL^{-1})	Linear Range (ng mL^{-1})	Detection Antibody	Detection Sample	Ref
1	chemiluminescence enzyme immunoassay	0.01	0.01–5	HRP-labeled anti-SEB mAbs	tap water, milk, human serum, etc.	[37]
2	chemiluminescence immunoassay	0.004	0.01–1	co-immobilizing HRP and anti-SEB mAbs on mesoporous silica nanoparticle	milk, water, and serum samples	[38]
3	electrochemical immunosensor	0.017	0.05–5	Anti-SEB mAbs @ magnetosome	milk	[39]
4	immunomagnetic-electrochemiluminescent immunoassay	0.001	0.1–100	Ruthenium(□) tris-bipyridine chelate-labeled anti-SEB mAbs	urine, serum, homogenates, and skim milk	[40]
5	chemiluminescent immunosensor	0.0033	0.006–0.564	HRP-labeled anti-SEB mAbs	serum, milk, lake water	[41]
6	chemiluminescence-based microarray immunoassay	0.1±0.1	1.7–48.6	Biotin-labeled anti-SEB mAbs	water	[42]

7	chemiluminescence multichannel immunosensor	0.0156	0.0156–100	Fluor555-labeled anti-SEB mAbs	milk	[43]
8	chemiluminescence lateral flow	0.00286	0.001–100	Anti-SEB magnetic quantum dot nanoparticles	PBS, milk, grape juice	[44]
9	chemiluminescent immunosensor	1.44	3.12–50	Anti-SEB Nb–ALP fusion protein	milk, drinking water, human serum	This method

3.6 Cross-reactivity and Thermostability

To evaluate the selectivity of our sandwich CLIA method, 50 ng/ml SEA, SEB, OVA, BSA, and IgG antibody, which were similar with one another, were used to determine selectivity. The cross-reactivity was calculated by the ratio of the chemiluminescence value of the similar protein to the chemiluminescence value of SEB; the final values were the means of three replicates. In these results (Figure 10), the cross-reactivity of SEA, OVA, BSA and IgG gave a similar value to that of the blank control group, indicating that the Nb37–ALP exhibited better selectivity while also showing some nonspecific protein adsorption.

The endurance of Nb37–ALP in high temperatures is crucially important to its ability to function. We tested this by placing Nb37–ALP at 37 □, 60 □, 80 ℃ for 120 min, and analyzing the binding activity at 0, 30, 60 and 120 min using sandwich CLIA with 50 ng mL^{-1} SEB. As shown in Figure 11, the binding activity of Nb37–ALP had slightly reduced after 30 min at 37 ℃, while it had reduced about 25% after 120 min. At 60 ℃, the binding retained 84% of its original activity after 30 min, and had retained 63% of its activity after 120 min. In previous studies [45-47], nanobodies retained 80%–100% of its activity after 5 min heating at 60 ℃. Further, in studies on the thermostability of ALP [48] and Nb–ALP fusion protein [34], Nb–ALP fusion protein showed perfect thermostability, retaining 80% of its activity after 30 min heating at 70 ℃. These data demonstrate the thermostability of nanobodies and Nb–ALP fusion protein, ensuring the potential of their application under harsh conditions.

3.7 Recovery Analysis of Spiked Samples

Performance of each newly developed analytical method should be evaluated using real samples and assessed by comparing the concentration of SEB as determined by the developed method and that determined by the ELISA technique. As shown in Table 2, the recoveries determined by commercial ELISA ranged from 81.6%–90.2%, while the recoveries determined by this method ranged from 82.5%–95.2%. Thus, the data indicate that these two methods have a similar efficiency. At the same time, in the serum samples, there were protein levels (including some anti-SEB antibodies) that might lead to nonspecific adsorption of Nb–ALP and loss of SEB, thus reducing the recovery achieved by this method.

4 Conclusion

In this study, we obtained an SEB-binding Nb37 from a naïve phage-display library. Then, Nb–ALP fusion protein was constructed and obtained. A rapid and sensitive sandwich CLIA for detecting SEB was developed using Nb37–ALP as the detecting antibody. The Nb–ALP fusion protein, which combined detection and report, was soluble, thermally stable and able to be easily prepared while maintaining a stable performance at a low cost. The fusion protein in sandwich CLIA also reduced

analysis time and enhanced sensitivity, while avoiding the chemically coupled probe. Further, the interaction between SEB and Nb37 was analyzed and validated by molecular modeling. The results showed that the CDR3 of Nb37 embedded itself in the space generated by the and MHC- and TcR-binding sites of SEB. The Arg101, Arg102, and Phe103 of Nb37 formed six salt-bridges with Val152, Asn157 and Asn186 of the SEB, and these bridges were critical for the specificity of complex formation. Altogether, these results indicate Nb37–ALP is a valuable tool for fast and sensitive detection of SEB toxin, and that nanobodies could also be promising for use in detecting proteins.

Declarations of interest

The authors have no conflicts of interest to declare.

Funding

This study was financially supported in part by The Major Research Plan of the National Natural Science Foundation of China (Grant No. 2018YFC1602903, Grant No. 2018YFC1602904) and the Municipal Key Program of Natural Science Foundation of Tianjin (Grant No. 17JCZDJC34500).

References

[1] S. Wu, N. Duan, H. Gu, L. Hao, H. Ye, W. Gong, Z. Wang, A review of the methods for detection of staphylococcus aureus enterotoxins, Toxins (Basel) 8(7) (2016).

[2] I.V. Pinchuk, E.J. Beswick, V.E. Reyes, Staphylococcal enterotoxins, Toxins (Basel) 2(8) (2010) 2177-2197.

[3] D. Zhou, G. Xie, X. Cao, X. Chen, X. Zhang, H. Chen, Colorimetric determination of staphylococcal enterotoxin B via DNAzyme-guided growth of gold nanoparticles, Microchim Acta 183(10) (2016) 2753-2760.

[4] M. Labib, M. Hedstrom, M. Amin, B. Mattiasson, A capacitive biosensor for detection of staphylococcal enterotoxin B, Anal Bioanal Chem 393(5) (2009) 1539-1544.

[5] J. Hwang, S. Lee, J. Choo, Application of a SERS-based lateral flow immunoassay strip for the rapid and sensitive detection of staphylococcal enterotoxin B, Nanoscale 8(22) (2016) 11418-11425.

[6] Z. Wu, D. He, B. Cui, A fluorometric assay for staphylococcal enterotoxin B by making use of platinum coated gold nanorods and of upconversion nanoparticles, Mikrochim Acta 185(11) (2018) 516.

[7] W. Wang, W. Wang, L. Liu, L. Xu, H. Kuang, J. Zhu, C. Xu, Nanoshell-Enhanced Raman Spectroscopy on a Microplate for Staphylococcal Enterotoxin B Sensing, ACS Appl Mater Interfaces 8(24) (2016) 15591-15597.

[8] P. Xue, Y. Li, Z. Zhang, A. Fu, F. Liu, X. Zhang, Y. Sun, L. Chen, B. Jin, K. Yang, Novel chemiluminescent assay for staphylococcal enterotoxin B, Microchim Acta 174(1-2) (2011) 167-174.

[9] J. Achuth, R.M. Renuka, K. Jalarama Reddy, M.S. Shivakiran, M. Venkataramana, K. Kadirvelu, Development and evaluation of an IgY based silica matrix immunoassay platform for rapid onsite SEB detection, RSC Adv 8(45) (2018) 25500-25513.

[10] A. Szkola, E.M. Linares, S. Worbs, B.G. Dorner, R. Dietrich, E. Martlbauer, R. Niessner, M. Seidel, Rapid and simultaneous detection of ricin, staphylococcal enterotoxin B and saxitoxin by chemiluminescence-based microarray immunoassay, Analyst 139(22) (2014) 5885-5892.

[11] L. Chen, Z. Zhang, X. Zhang, A. Fu, P. Xue, R. Yan, A novel chemiluminescence immunoassay of staphylococcal enterotoxin B using HRP-functionalised mesoporous silica nanoparticle as label, Food Chem 135(1) (2012) 208-212.

[12] A. Sharma, V.K. Rao, D.V. Kamboj, R. Gaur, S. Upadhyay, M. Shaik, Relative efficiency of zinc sulfide (ZnS) quantum dots (QDs) based electrochemical and fluorescence immunoassay for the detection of staphylococcal enterotoxin B (SEB), Biotechnol Rep (Amst) 6 (2015) 129-136.

[13] D. Tang, J. Tang, B. Su, G. Chen, Ultrasensitive electrochemical immunoassay of staphylococcal enterotoxin B in food using enzyme-nanosilica-doped carbon nanotubes for signal amplification, J Agric Food Chem 58(20) (2010) 10824-10830.

[14] Z. Sun, J. Lv, X. Liu, Z. Tang, X. Wang, Y. Xu, B.D. Hammock, Development of a nanobody-avitag fusion protein and its application in a streptavidin-biotin-amplified enzyme-linked immunosorbent assay for ochratoxin A in Cereal, Anal Chem 90(17) (2018) 10628-10634.

[15] H. Oyama, E. Tanaka, T. Kawanaka, I. Morita, T. Niwa, N. Kobayashi, Anti-idiotype scFv-enzyme fusion proteins: a clonable analyte-mimicking probe for standardized immunoassays targeting small biomarkers, Anal Chem 85(23) (2013) 11553-11559.

[16] S. Steeland, R.E. Vandenbroucke, C. Libert, Nanobodies as therapeutics: big opportunities for small antibodies, Drug Discov Today 21(7) (2016) 1076-1113.

[17] T. De Meyer, S. Muyldermans, A. Depicker, Nanobody-based products as research and diagnostic tools, Trends Biotechnol 32(5) (2014) 263-270.

[18] C.S. Bever, J.X. Dong, N. Vasylieva, B. Barnych, Y.L. Cui, Z.L. Xu, B.D. Hammock, S.J. Gee, VHH antibodies: emerging reagents for the analysis of environmental chemicals, Anal Bioanal Chem 408(22) (2016) 5985-6002.

[19] G. Gonzalez-Sapienza, M.A. Rossotti, S. Tabares-da Rosa, Single-domain antibodies as versatile affinity reagents for analytical and diagnostic applications, Front Immunol 8 (2017) 977.

[20] M.A. Rossotti, M. Pirez, A. Gonzalez-Techera, Y.L. Cui, C.S. Bever, K.S.S. Lee, C. Morisseau, C. Leizagoyen, S. Gee, B.D. Hammock, G. Gonzalez-Sapienza, Method for sorting and pairwise selection of nanobodies for the development of highly sensitive sandwich immunoassays, Anal Chem 87(23) (2015) 11907-11914.

[21] S. Muyldermans, T.N. Baral, V.C. Retamozzo, P. De Baetselier, E. De Genst, J. Kinne, H. Leonhardt, S. Magez, V.K. Nguyen, H. Revets, U. Rothbauer, B. Stijlemans, S. Tillib, U. Wernery, L. Wyns, G. Hassanzadeh-Ghassabeh, D. Saerens, Camelid immunoglobulins and nanobody technology, Vet Immunol Immunopathol 128(1-3) (2009) 178-183.

[22] M. Yamagata, J.R. Sanes, Reporter-nanobody fusions (RANbodies) as versatile, small, sensitive immunohistochemical reagents, Proc Natl Acad Sci USA 115(9) (2018) 2126-2131.

[23] M. Shu, Y. Xu, D. Wang, X. Liu, Y.P. Li, Q.H. He, Z. Tu, Y.L. Qiu, Y.W. Ji, X.X. Wang, Anti-idiotypic nanobody: A strategy for development of sensitive and green immunoassay for Fumonisin B-1, Talanta 143 (2015) 388-393.

[24] S. Yang, Y. Shang, S. Yin, D. Wang, J. Cai, Z. Gong, M. Serge, X. Liu, A phage-displayed single domain antibody fused to alkaline phosphatase for detection of porcine circovirus type 2, J Virol Methods 213 (2015) 84-92.

[25] Z. Tang, X. Wang, J. Lv, X. Hu, X. Liu, One-step detection of ochratoxin A in cereal by dot immunoassay using a nanobody-alkaline phosphatase fusion protein, Food Control 92 (2018) 430-436.

[26] J.C. Frei, J.R. Lai, Protein and antibody engineering by phage display, Methods Enzymol 580 (2016) 45-87.

[27] B. Webb, A. Sali, Comparative protein structure modeling using MODELLER, Curr Protoc Bioinformatics 54 (2016) 5.6.1-5.6.37.

[28] P.D. Skottrup, Structural insights into a high affinity nanobody:antigen complex by homology modelling, J Mol Graph Model 76 (2017) 305-312.

[29] A.C. Papageorgiou, H.S. Tranter, K.R. Acharya, Crystal structure of microbial superantigen staphylococcal enterotoxin B at 1.5 A resolution: implications for superantigen recognition by MHC class II molecules and T-cell receptors, J Mol Biol 277(1) (1998) 61-79.

[30] C. Wang, P. Bradley, D. Baker, Protein-protein docking with backbone flexibility, J Mol Biol 373(2) (2007) 503-519.

[31] D. Seeliger, B.L. de Groot, Ligand docking and binding site analysis with PyMOL and Autodock/Vina, J Comput Aid Mol Des 24(5) (2010) 417-22.

[32] E.H. Baugh, L. Sergey, B.D. Weitzner, J.J. Gray, Real-time PyMOL visualization for Rosetta and PyRosetta, Plos One 6(8) (2011) e21931.

[33] K. He, F. Wei, X. Zhang, J. Li, D. Zhang, D. Wei, Production and characterization of a single-chain Fv antibody–alkaline phosphatase fusion protein specific for ampicillin, Food Agr Immunol 30(1) (2018) 1-12.

[34] J.L. Liu, D. Zabetakis, A.B. Lee, E.R. Goldman, G.P. Anderson, Single domain antibody–alkaline phosphatase fusion proteins for antigen detection — Analysis of affinity and thermal stability of single domain antibody, J Immunol Methods 393(1-2) (2013) 1-7.

[35] W. Mandecki, M.A. Shallcross, J. Sowadski, S. Tomazic-Allen, Mutagenesis of conserved residues within the active site of *Escherichia coli* alkaline phosphatase yields enzymes with increased kcat, Protein Eng Des Sel 4(7) (1991) 801-804.

[36] S. Muyldermans, V.V. Smider, Distinct antibody species: structural differences creating therapeutic opportunities, Curr Opin Immunol 40 (2016) 7-13.

[37] F. Liu, Y. Li, C. Song, B. Dong, Z. Liu, K. Zhang, H. Li, Y. Sun, Y. Wei, A. Yang, Highly sensitive microplate chemiluminescence enzyme immunoassay for the determination of staphylococcal enterotoxin B based on a pair of specific monoclonal antibodies and its application to various matrices, Anal Chem 82(18)(2010) 7758-7765.

[38] L. Chen, Z. Zhang, X. Zhang, A. Fu, P. Xue, R. Yan, A novel chemiluminescence immunoassay of staphylococcal enterotoxin B using HRP-functionalised mesoporous silica nanoparticle as label, Food Chem 135(1)(2012).

[39] L. Wu, B. Gao, F. Zhang, X. Sun, Y. Zhang, Z. Li, A novel electrochemical immunosensor based on magnetosomes for detection of staphylococcal enterotoxin B in milk, Talanta106 (2013) 360-366.

[40] T.M. Kijek, C.A. Rossi, D. Moss, R.W. Parker, E.A. Henchal, Rapid and sensitive immunomagnetic-electrochemiluminescent detection of staphyloccocal enterotoxin B, J Immunol Methods 236(1-2) (2000) 9-17.

[41] P. Xue, Y. Li, Z. Zhang, A. Fu, F. Liu, X. Zhang, Y. Sun, L. Chen, B. Jin, K. Yang, Novel chemiluminescent assay for staphylococcal enterotoxin B, Microchim Acta 174(1-2)(2011) 167-174.

[42] A. Szkola, E.M. Linares, S. Worbs, B.G. Dorner, R. Dietrich, E. Martlbauer, R. Niessner, M. Seidel, Rapid and simultaneous detection of ricin, staphylococcal enterotoxin B and saxitoxin by chemiluminescence-based microarray immunoassay, Analyst 139(22) (2014) 5885-5892.

[43] T. Kasama, M. Ikami, W. Jin, K. Yamada, N. Kaji, Y. Atsumi, M. Mizutani, A. Murai, A. Okamoto, T. Namikawa, M. Ohta, M. Tokeshi, Y. Baba, Rapid, highly sensitive, and simultaneous detection of staphylococcal enterotoxins in milk by using immuno-pillar devices, Anal Methods 7(12) (2015) 5092-5095.

[44] C. Wang, R. Xiao, S. Wang, X. Yang, Z. Bai, X. Li, Z. Rong, B. Shen, S. Wang, Magnetic quantum dot based lateral flow assay biosensor for multiplex and sensitive detection of protein toxins in food samples, Biosens Bioelectron 146 (2019) 111754-111754.

[45] Y.L. Qiu, Q.H. He, Y. Xu, A.K. Bhunia, Z. Tu, B. Chen, Y.Y. Liu, Deoxynivalenol-mimic nanobody isolated from a naive phage display nanobody library and its application in immunoassay, Anal Chim Acta 887 (2015) 201-208.

[46] T. He, Y. Wang, P. Li, Q. Zhang, J. Lei, Z. Zhang, X. Ding, H. Zhou, W. Zhang, Nanobody-based enzyme immunoassay for aflatoxin in agro-products with high tolerance to cosolvent methanol, Anal Chem 86(17) (2014) 8873-8880.

[47] J. Chen, Q.H. He, Y. Xu, J.H. Fu, Y.P. Li, Z. Tu, D. Wang, M. Shu, Y.L. Qiu, H.W. Yang, Y.Y. Liu, Nanobody medicated immunoassay for ultrasensitive detection of cancer biomarker alpha-fetoprotein, Talanta 147 (2016) 523-530.

[48] O.M. Poltorak, E.S. Chukhrai, A.A. Kozlenkov, M.F. Chaplin, M.D. Trevan, The putative common mechanism for inactivation of alkaline phosphatase isoenzymes, J Mol Catal B-Enzym 7(1) (1999) 157-163.

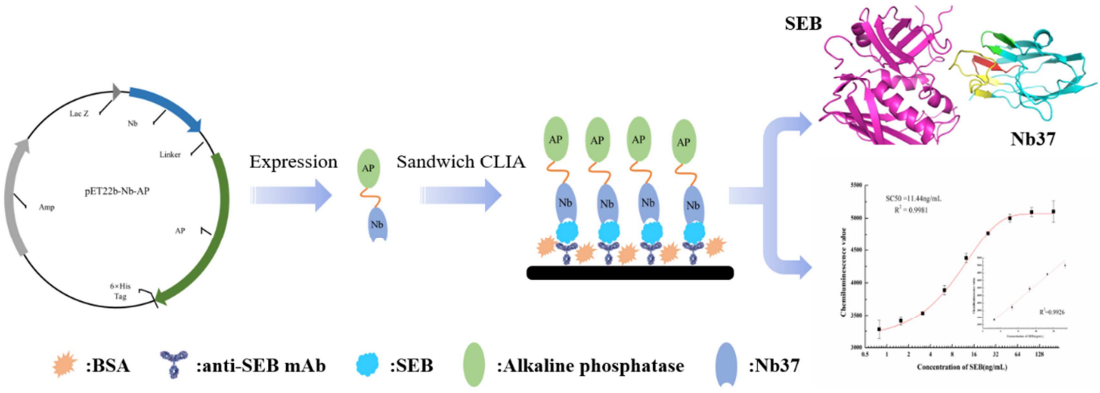

Graphical Abstract

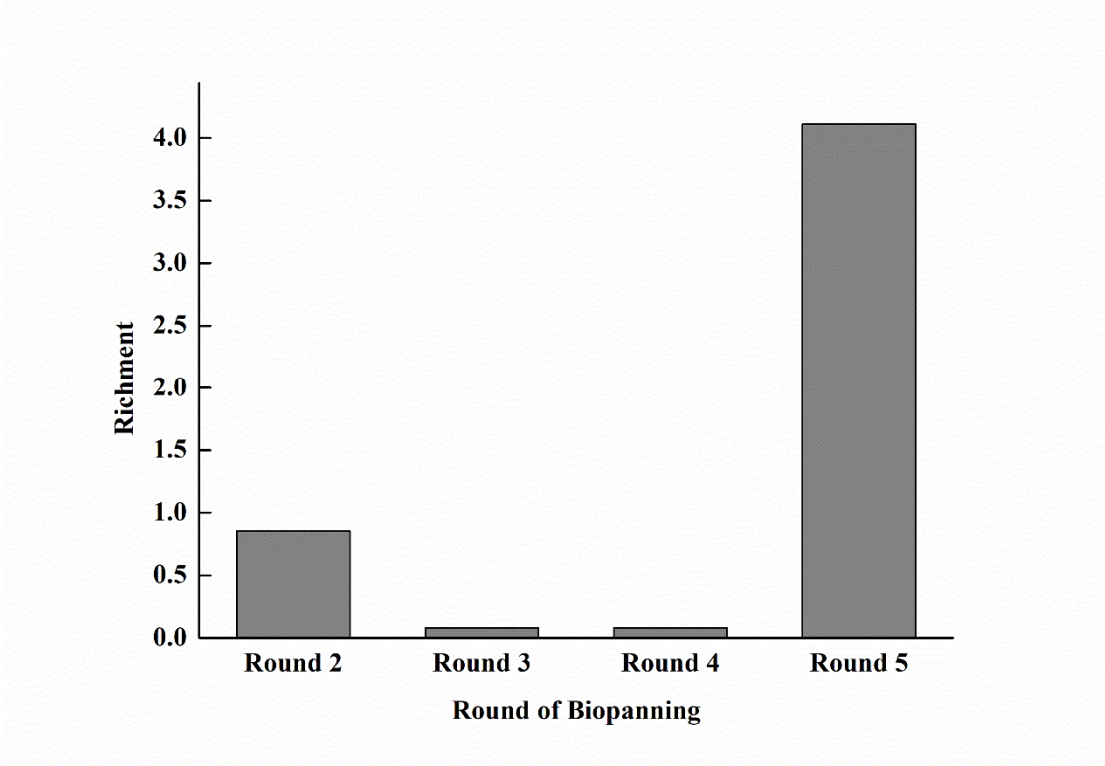

Figure. 1. Enrichment of phage-display nanobody in biopanning cycles.

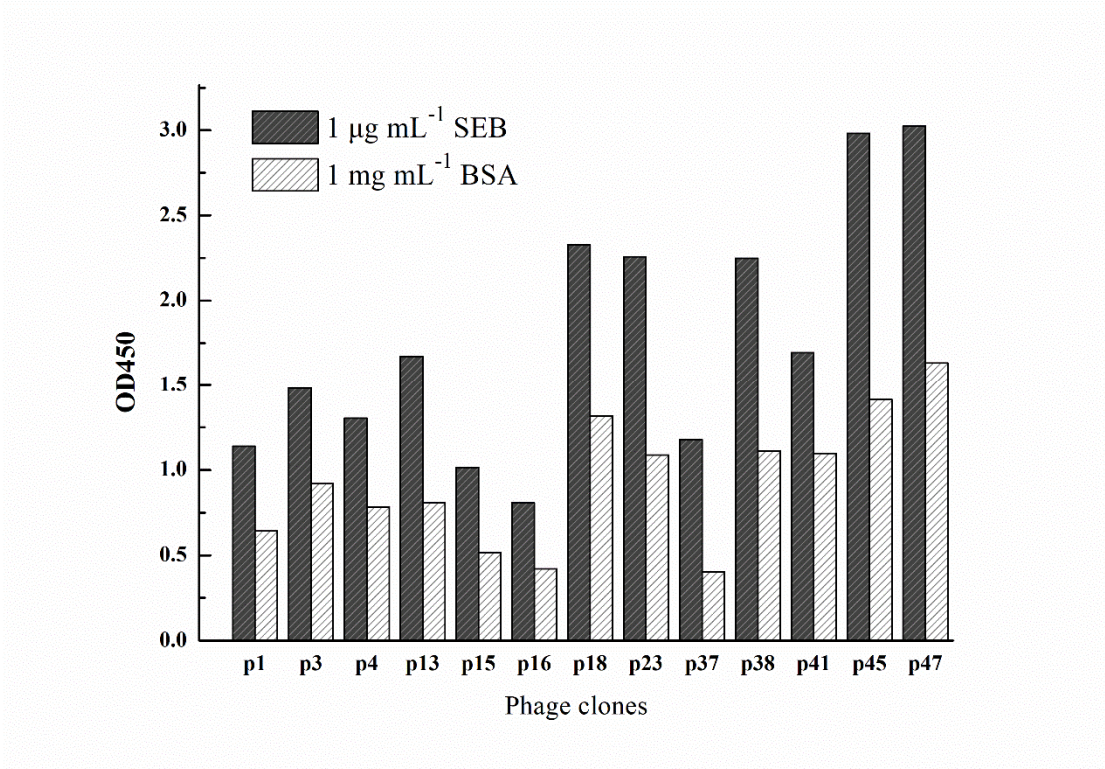

Figure. 2. Phage ELISA for identifying the positive clones binding to SEB.

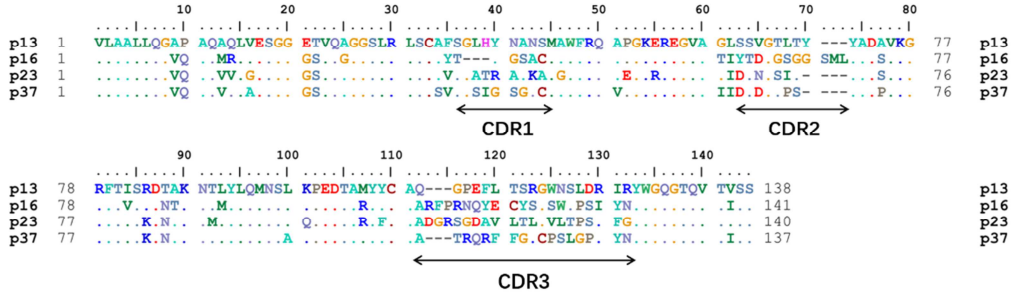

Figure. 3. Four kinds of different amino acid sequences of phage displayed nanobodies against SEB.

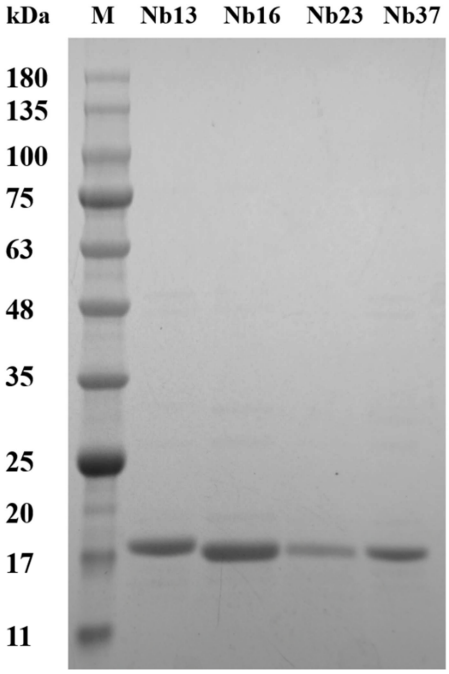

Figure. 4. SDS-PAGE analysis of nanobodies Nb-13, Nb-16, Nb-23 and Nb-37.

375

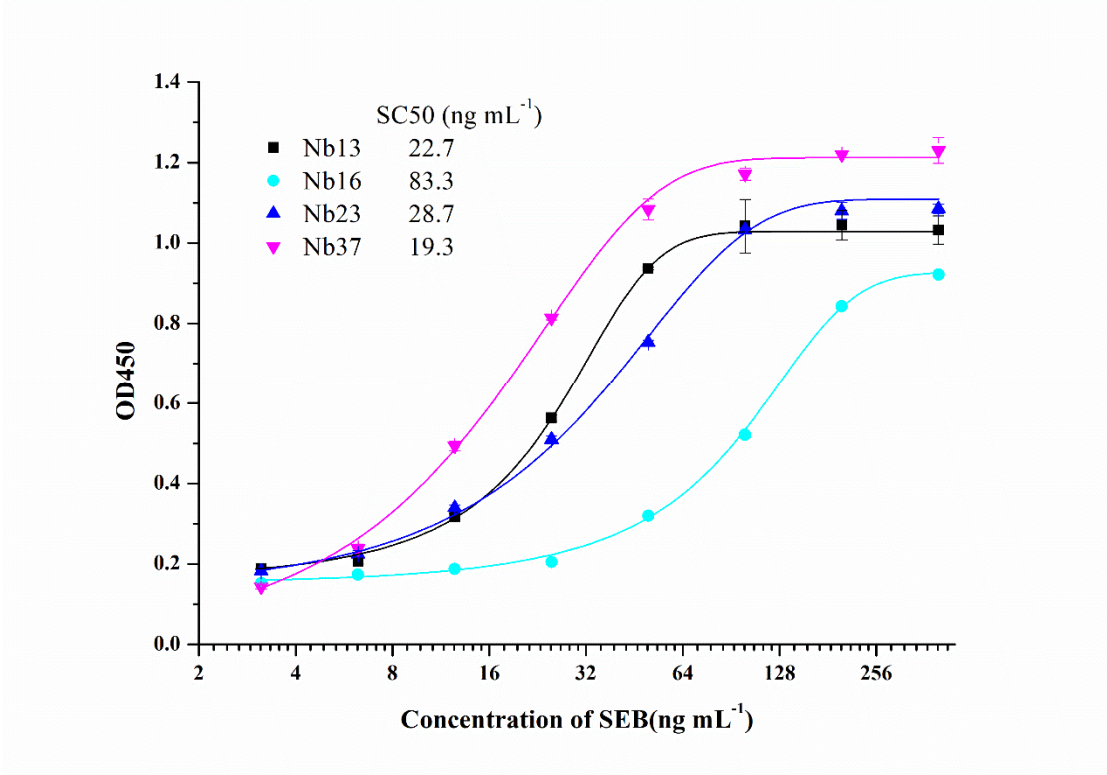

376

377 Figure. 5. Direct ELISA for SEB established with Nb-13, Nb-16, Nb-23 and Nb-37.

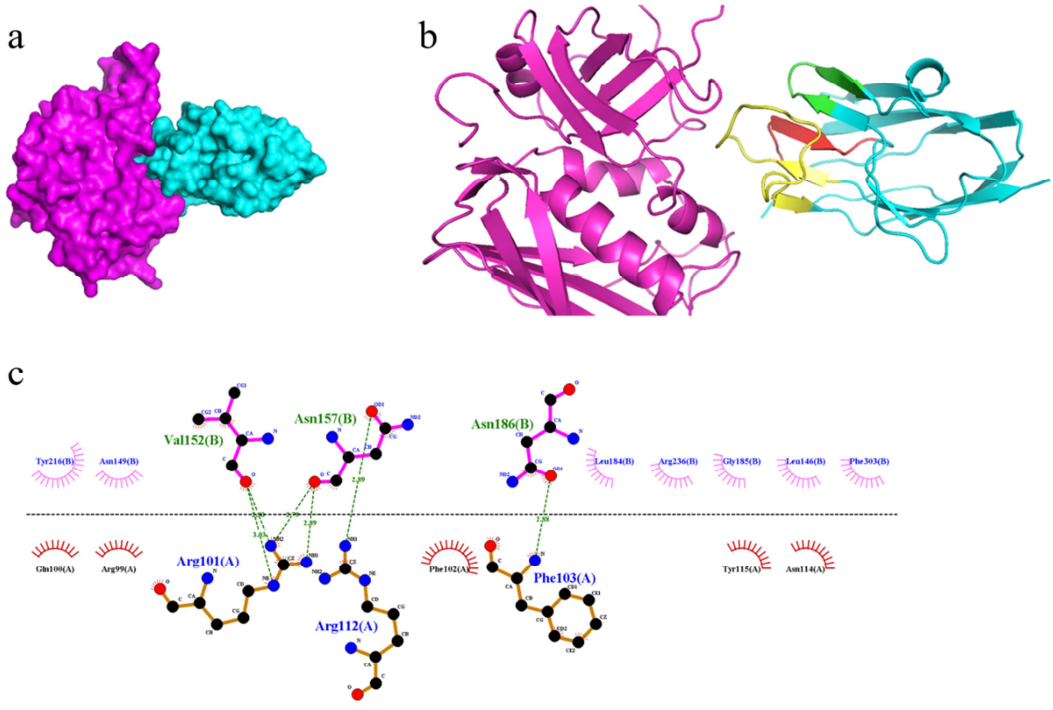

378

379 Figure. 6. Overall structure of SEB/Nb37 complex. a: view of the SEB/Nb37 complex is presented as a
380 surface presentation, the SEB is seen in magenta, the Nb37 in seen in cyan. b: view of the SEB/Nb37
381 complex is presented as a ribbon presentation, the SEB is seen in magenta, the Nb37 in seen in cyan, and

382 CDR3 of Nb37 is seen in yellow, CDR2 is seen in green, CDR1 is seen in red. c: the interaction between
383 SEB and Nb37, SEB is labeled as (B), Nb37 is labeled as (A).

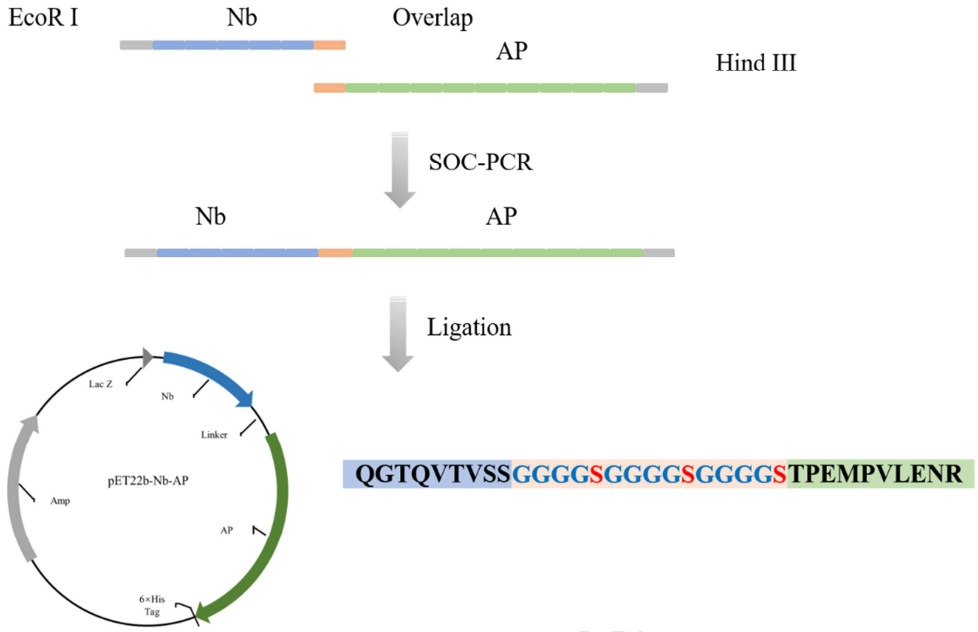

384

385 Figure. 7. Schematic of construction of Nb37-ALP, (G4S)3 peptides fragment was inverted as linker.

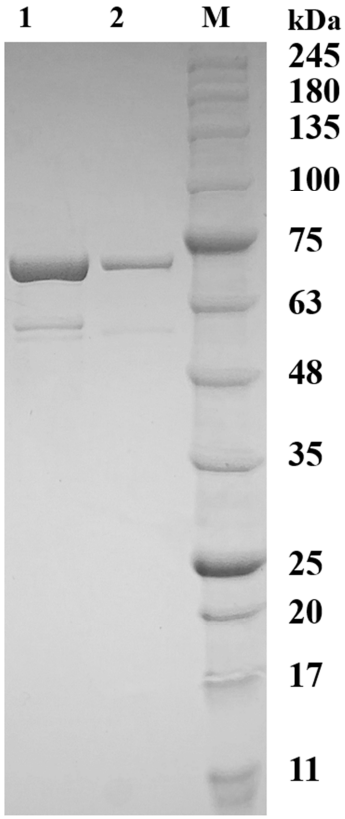

386

387 Figure. 8. SDS-PAGE analysis of Nb37-ALP fusion protein. Lane 1-2: the elution buffer with 240 mM
388 imidazole in 50 mM Tris-HCl(pH = 8.0).

389

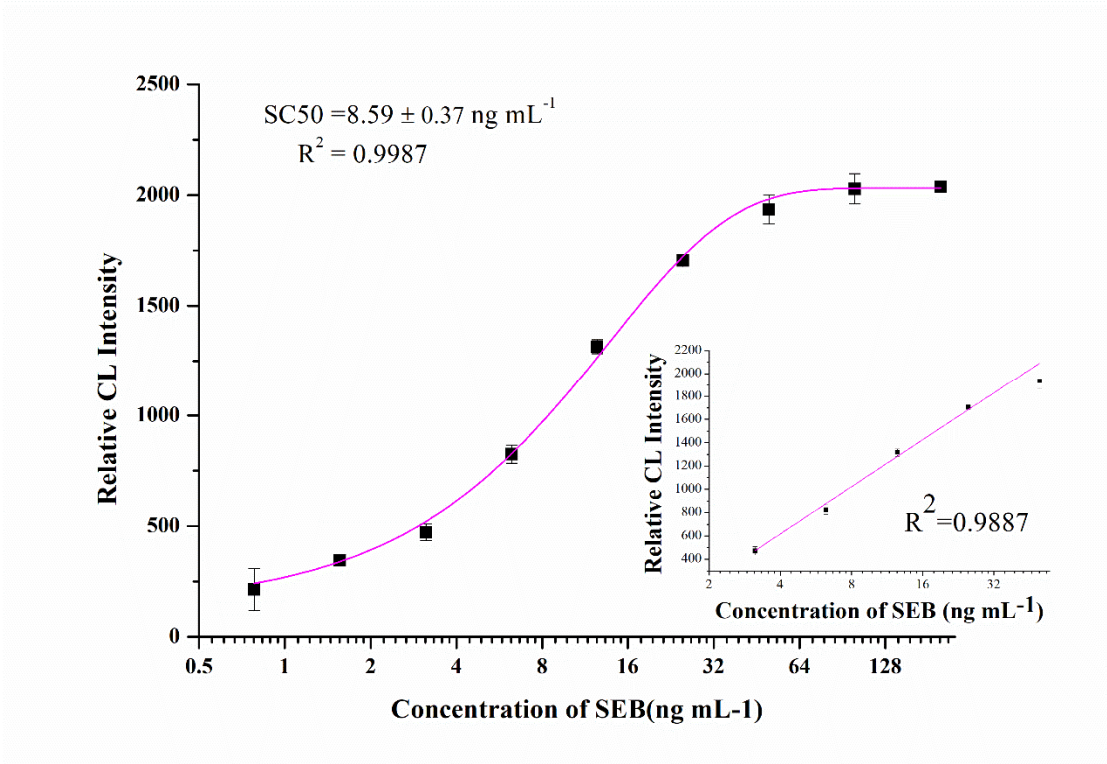

390

391 Figure. 9. Calibration curve of the sandwich CLIA for detection of SEB. Each value is the average of
392 three replicates and the standard deviations.

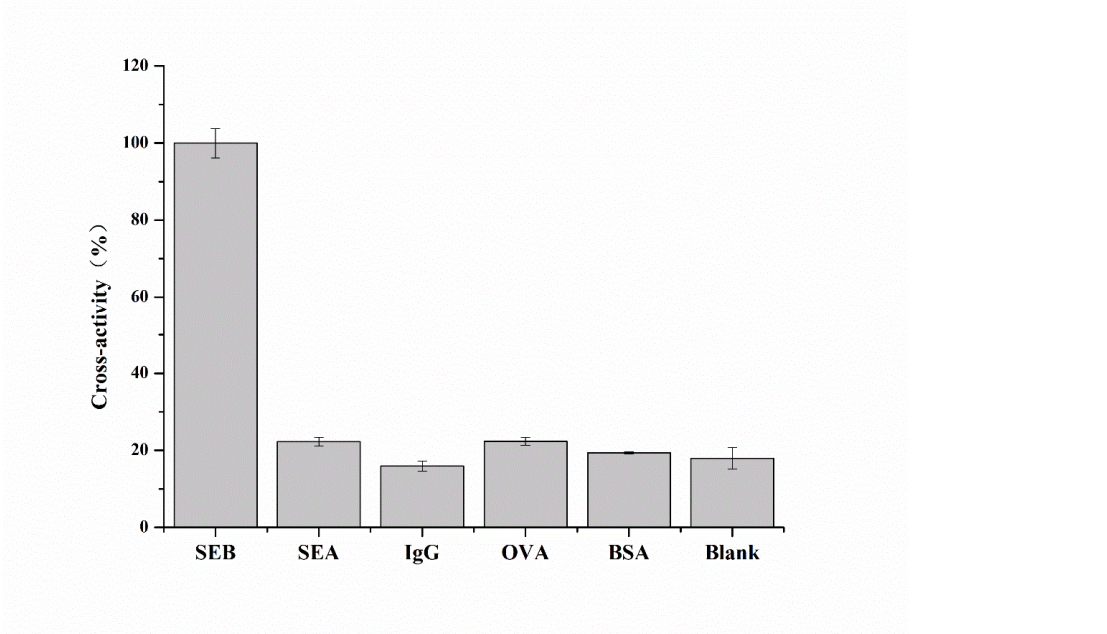

393

394 Figure. 10. Specificity of the sandwich CLIA for detection of SEB. Concentration of SEA, SEB, BSA,
395 OVA ang mouse IgG was at 50 ng mL^{-1}.

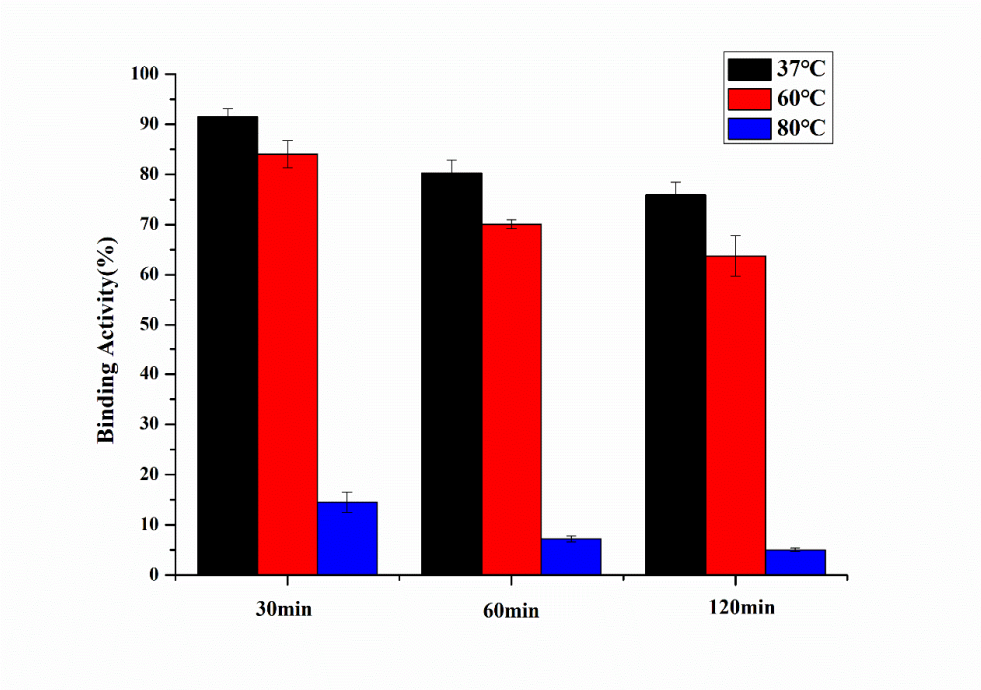

396

397 Figure. 11. Thermal stability analysis of Nb37-ALP at 37, 60, 80 □ for 30, 60 and 90 min in water-bath,
398 respectively.

399

400 Table 2. Recovery analysis of SEB in samples by ELISA kit and Nb37-ALP based sandwich CLIA

Sample	Found (ng mL^{-1})	Added (ng mL^{-1})	ELISA detection (ng mL^{-1})	Average recovery (%)	RSD(%)	CLIA detection (ng mL^{-1})	Average recovery (%)	RSD(%)
Pure milk	0.31	5	4.48	83.4	4.34	4.50	83.8	3.73
		10	8.79	84.8	1.06	8.92	86.1	2.45
		20	17.9	88.0	2.54	19.3	95.0	1.36
		40	36.2	89.6	9.65	38.4	95.2	2.06
Drinking water	0.13	5	4.28	83.0	4.96	4.45	86.4	2.95
		10	8.63	85.0	2.90	9.39	92.6	1.30
		20	17.8	88.4	2.71	18.9	93.9	4.02
		40	36.2	90.2	2.87	36.4	90.7	1.24
Serum	0.22	5	4.30	81.6	4.60	4.34	82.5	5.59
		10	8.88	86.6	2.52	8.83	86.1	4.24
		20	18.1	89.4	7.19	17.6	86.9	2.10
		40	36.3	90.2	6.00	35.2	88.5	2.23

Table 1 Immunoassays reported in the literature for the detection of SEB

No	Mechanism	Detection Limit (ng mL^{-1})	Linear Range (ng mL^{-1})	Detection Antibody	Detection Sample	Ref
1	chemiluminescence enzyme immunoassay	0.01	0.01–5	HRP-labeled anti-SEB mAbs	tap water, milk, human serum, etc.	[37]
2	chemiluminescence immunoassay	0.004	0.01–1	co-immobilizing HRP and anti-SEB mAbs on mesoporous silica nanoparticle	milk, water, and serum samples	[38]
3	electrochemical immunosensor	0.017	0.05–5	Anti-SEB mAbs @ magnetosome	milk	[39]
4	immunomagnetic-electrochemiluminescent immunoassay	0.001	0.1–100	Ruthenium(□) tris-bipyridine chelate-labeled anti-SEB mAbs	urine, serum, homogenates, and skim milk	[40]
5	chemiluminescent immunosensor	0.0033	0.006–0.564	HRP-labeled anti-SEB mAbs	serum, milk, lake water	[41]
6	chemiluminescence-based microarray immunoassay	0.1±0.1	1.7–48.6	Biotin-labeled anti-SEB mAbs	water	[42]
7	chemiluminescence multichannel immunosensor	0.0156	0.0156–100	Fluor 555-labeled anti-SEB mAbs	milk	[43]
8	chemiluminescence lateral flow	0.00286	0.001–100	Anti-SEB magnetic quantum dot nanoparticles	PBS, milk, grape juice	[44]
9	chemiluminescent immunosensor	1.44	3.12–50	Anti-SEB Nb–ALP fusion protein	milk, drinking water, human serum	This method

Table 2. Recovery analysis of SEB in samples by ELISA kit and Nb37-ALP based sandwich CLIA

Sample	Found (ng mL^{-1})	Added (ng mL^{-1})	ELISA detection (ng mL^{-1})	Average recovery(%)	RSD(%)	CLIA detection (ng mL^{-1})	Average recovery(%)	RSD(%)
Pure milk	0.31	5	4.48	83.4	4.34	4.50	83.8	3.73
		10	8.79	84.8	1.06	8.92	86.1	2.45
		20	17.9	88.0	2.54	19.3	95.0	1.36
		40	36.2	89.6	9.65	38.4	95.2	2.06
Drinking water	0.13	5	4.28	83.0	4.96	4.45	86.4	2.95
		10	8.63	85.0	2.90	9.39	92.6	1.30
		20	17.8	88.4	2.71	18.9	93.9	4.02
		40	36.2	90.2	2.87	36.4	90.7	1.24
Serum	0.22	5	4.30	81.6	4.60	4.34	82.5	5.59
		10	8.88	86.6	2.52	8.83	86.1	4.24
		20	18.1	89.4	7.19	17.6	86.9	2.10
		40	36.3	90.2	6.00	35.2	88.5	2.23

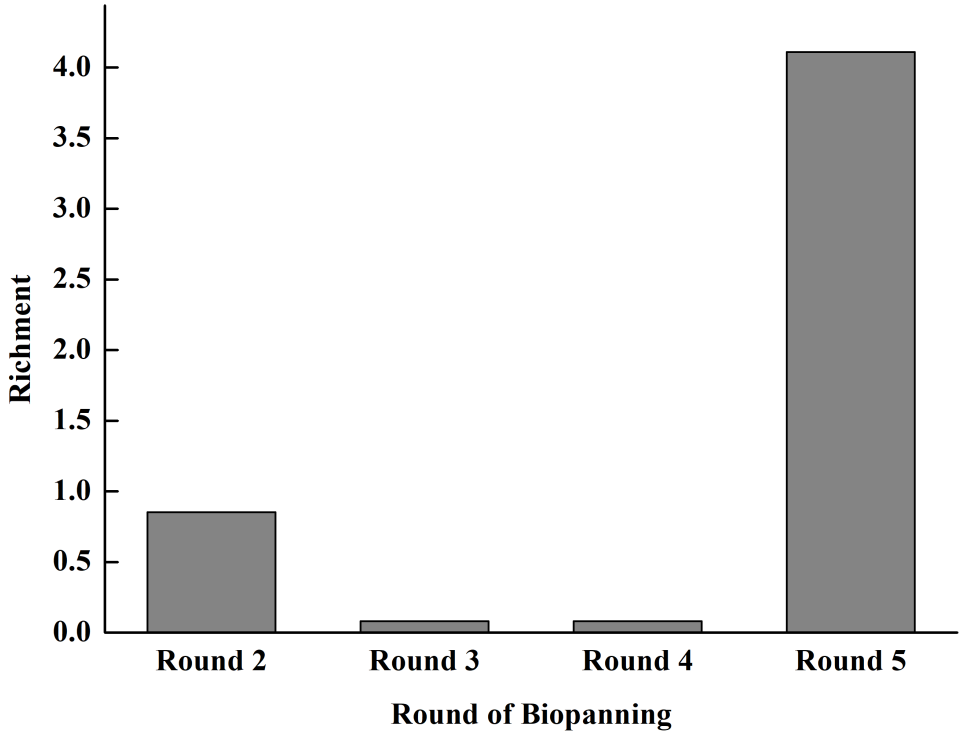
Richment
4.0
3.5
3.0
2.5
2.0
1.5
1.0
0.5
0.0
Round 2
Round 3
Round 4
Round 5
Round of Biopanning

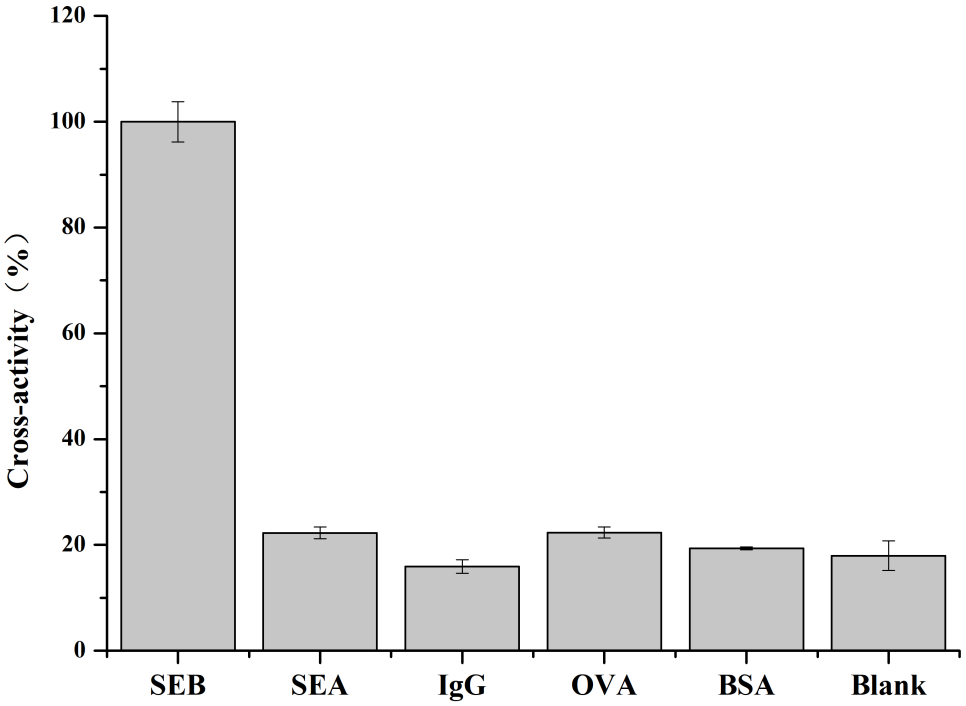

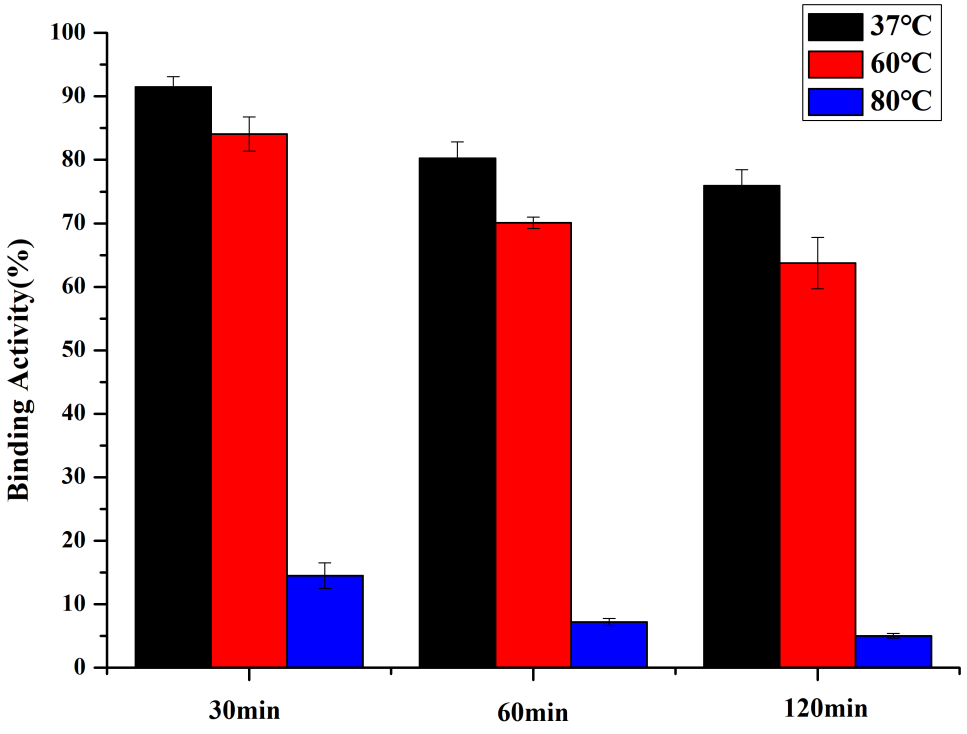
37°C
60°C
80°C
Binding Activity(%)
100
90
80
70
60
50
40
30
20
10
0
30min
60min
120min

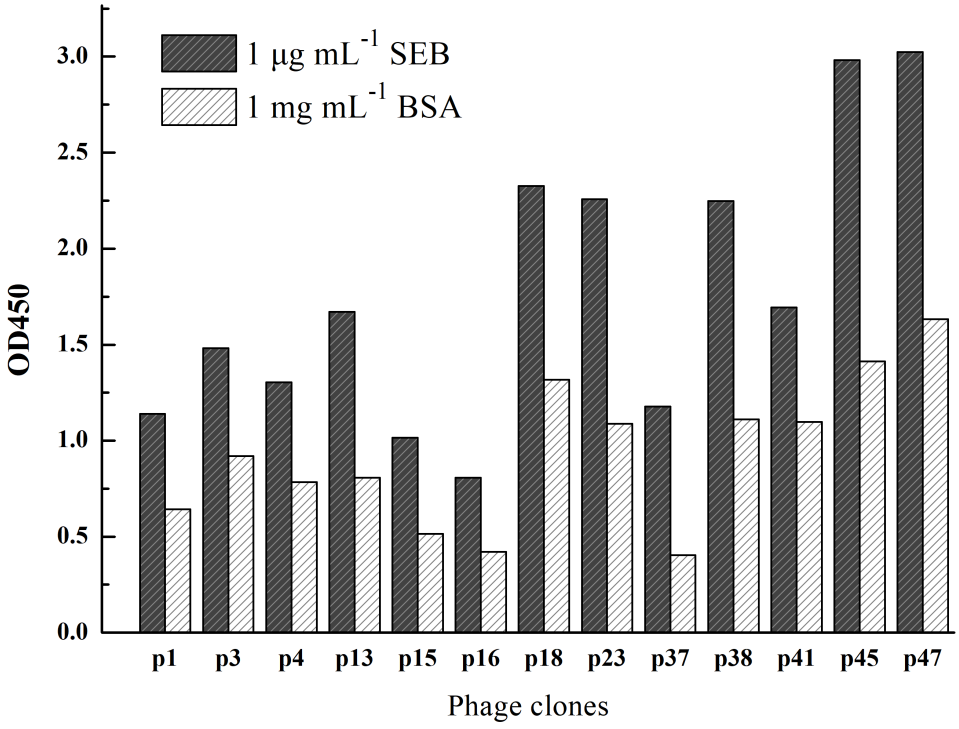
1 μg mL-1 SEB
1 mg mL-1 BSA
OD450
3.0
2.5
2.0
1.5
1.0
0.5
0.0
p1
p3
p4
p13
p15
p16
p18
p23
p37
p38
p41
p45
p47
Phage clones

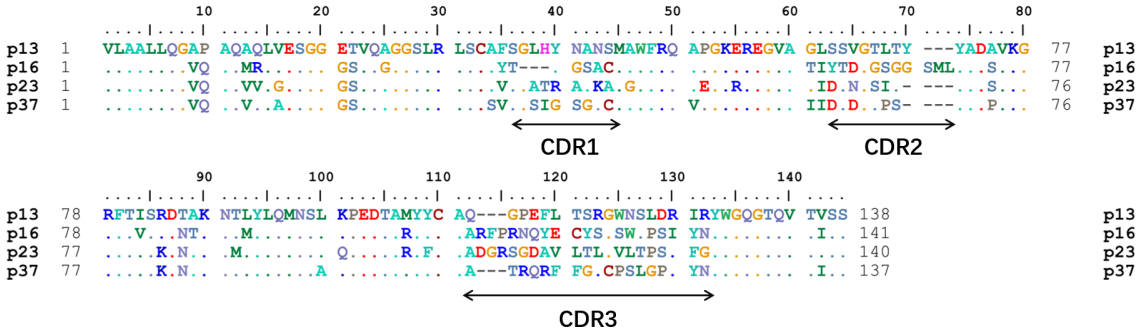

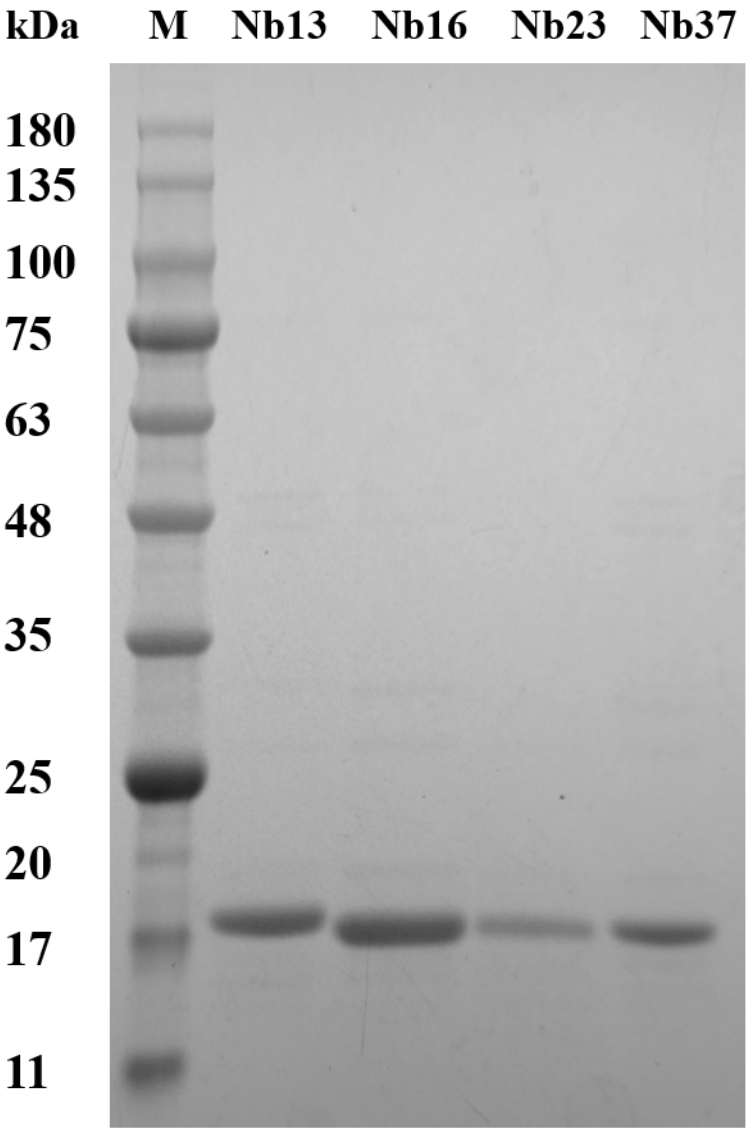
kDa
M
Nb13
Nb16
Nb23
Nb37
180
135
100
75
63
48
35
25
20
17
11

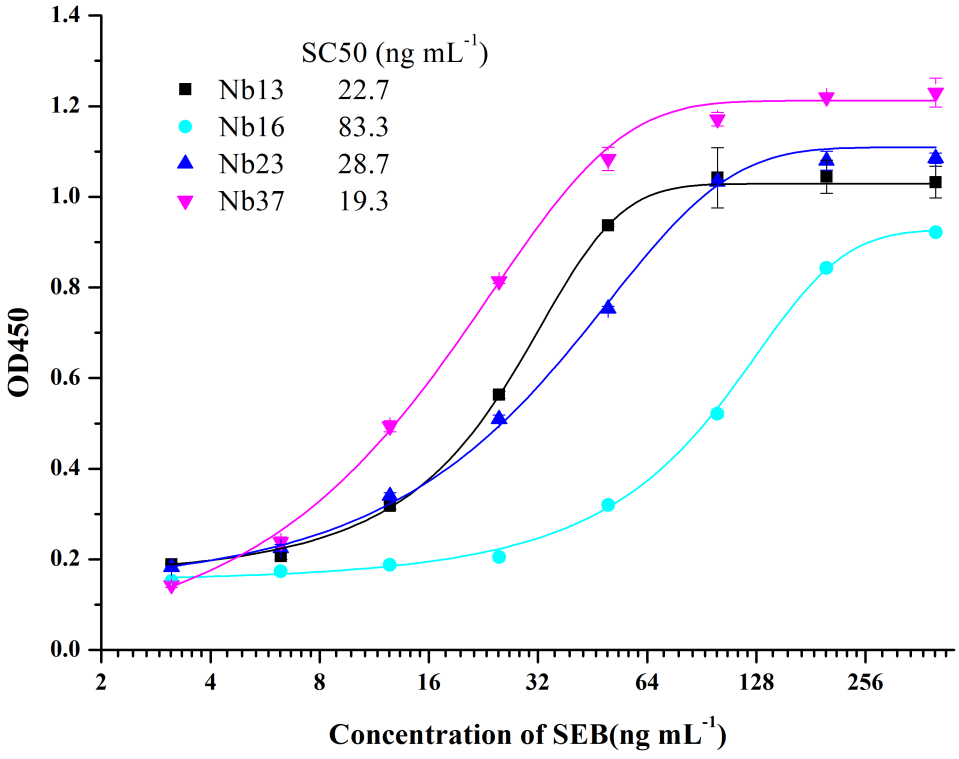
SC50 (ng mL-1)
Nb13 22.7
Nb16 83.3
Nb23 28.7
Nb37 19.3
OD450
1.4
1.2
1.0
0.8
0.6
0.4
0.2
0.0
2
4
8
16
32
64
128
256
Concentration of SEB(ng mL-1)

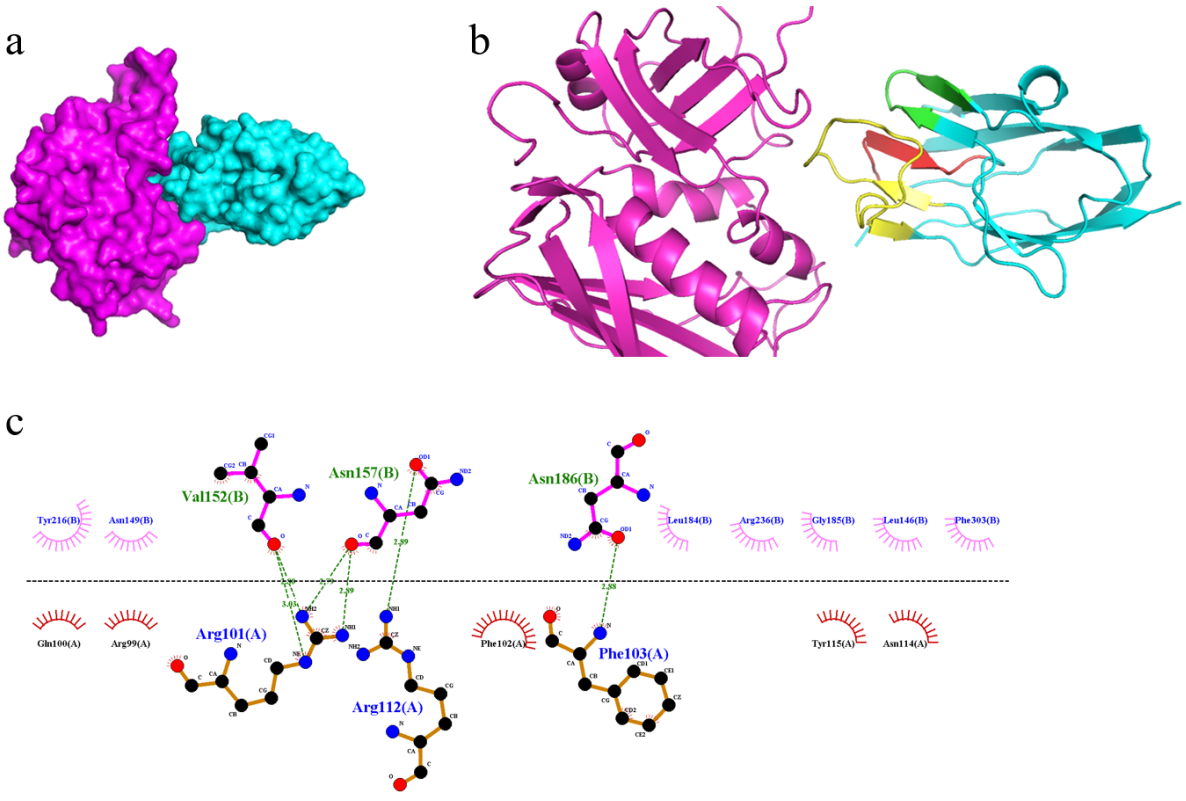
a
b
c
Tyr216(B)
Asn149(B)
Val152(B)
Asn157(B)
Asn186(B)
Leu184(B)
Arg236(B)
Gly185(B)
Leu146(B)
Phe303(B)
Gln100(A)
Arg99(A)
Arg101(A)
Arg112(A)
Phe102(A)
Phe103(A)
Tyr115(A)
Asn114(A)

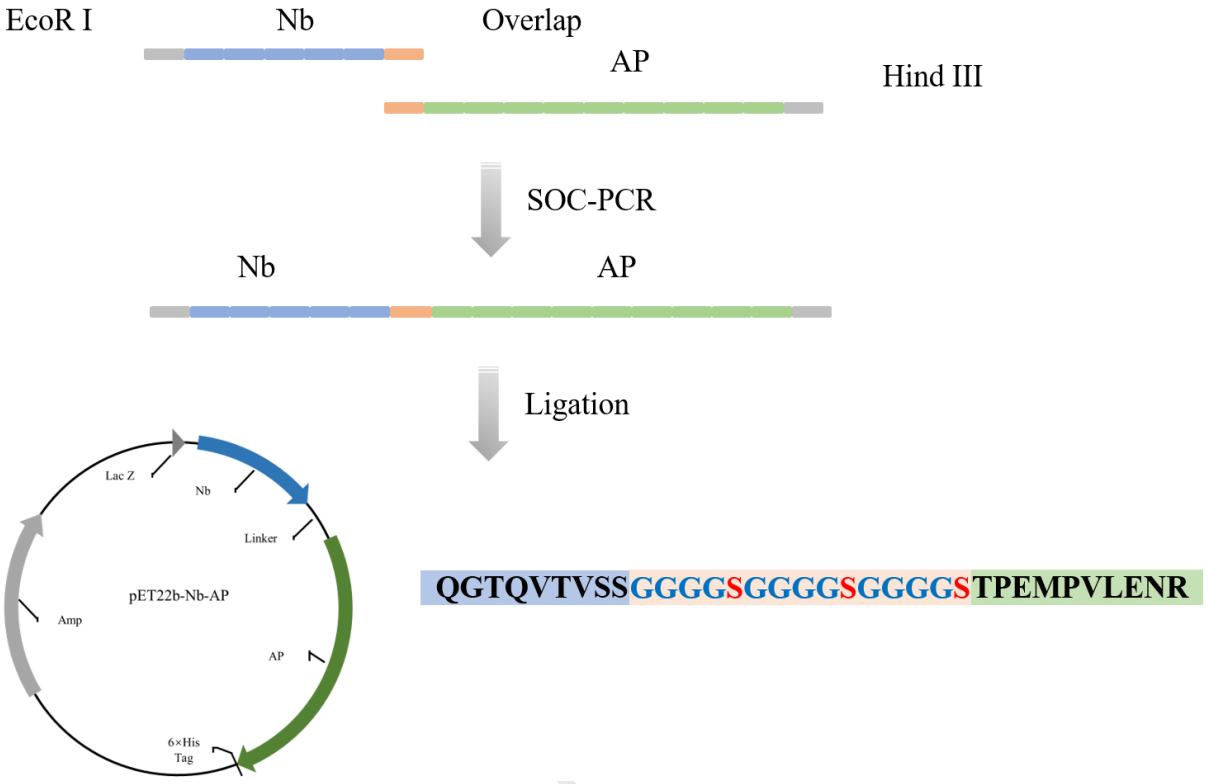
EcoR I
Nb
Overlap
AP
Hind III
SOC-PCR
Nb
AP
Ligation
Lac Z
Nb
Linker
pET22b-Nb-AP
Amp
AP
6×His Tag
QGTQVTVSSGGGGSGGGGSGGGGSTPEMPVLENR

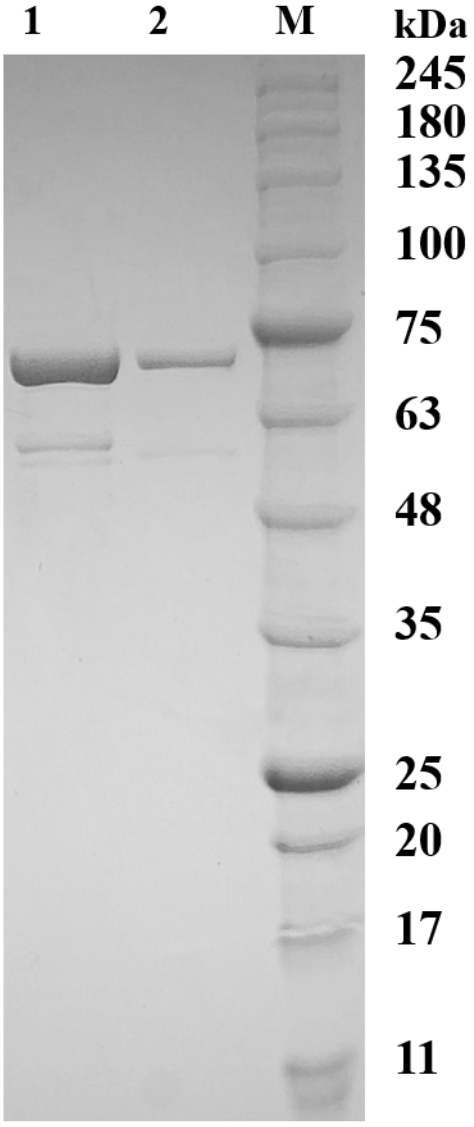

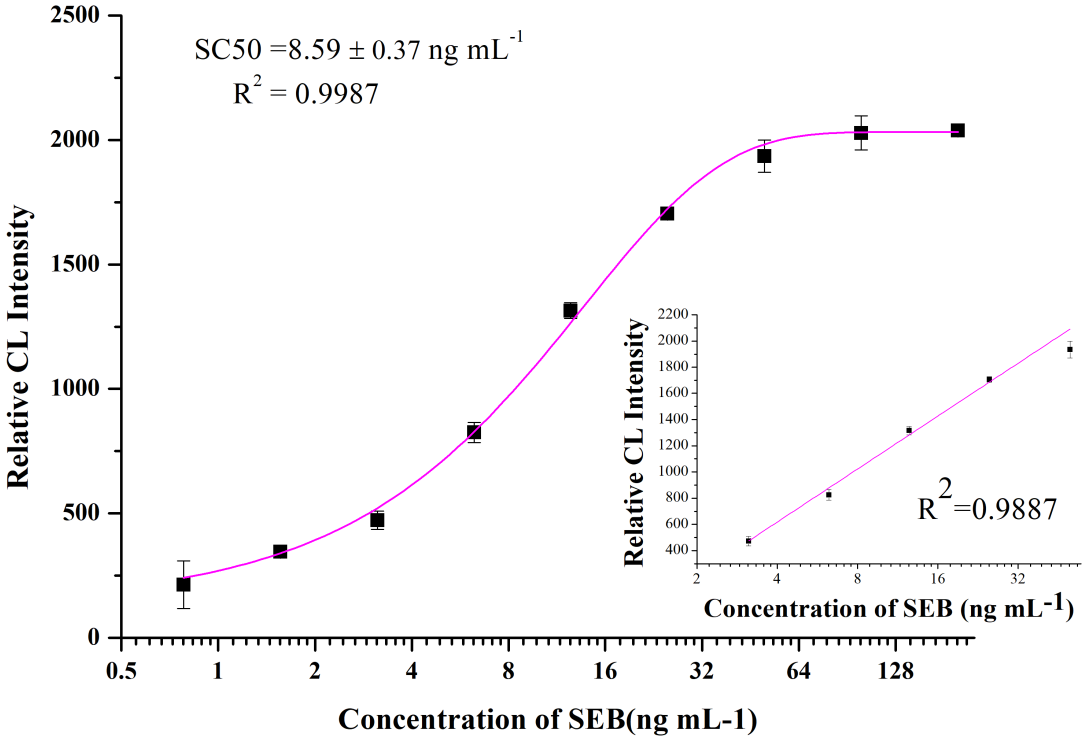
SC50 =8.59 ± 0.37 ng mL-1
R2 = 0.9987
Relative CL Intensity
Concentration of SEB(ng mL-1)
0
500
1000
1500
2000
2500
0.5
1
2
4
8
16
32
64
128
Relative CL Intensity
Concentration of SEB (ng mL-1)
R2=0.9887
400
600
800
1000
1200
1400
1600
1800
2000
2200
2
4
8
16
32

Highlights:

Nanobodies that bind to SEB were isolated from a naïve library

The molecular mechanism of nanobodies interacting with SEB was described

Nb37–ALP has the potential to replace chemically-coupled detection antibodies

Nb37–ALP was shown to be thermally stable and be able to be produced in large scale

A quick and sensitive sandwich CLIA method for the detection of SEB was developed

Conflict of interest

The authors declared that they have no conflicts of interest to this work.

We declare that we do not have any commercial or associative interest that represents a conflict of interest in connection with the work submitted.